Proc. Natl. Acad. Sci. USA
Vol. 88, pp. 3897–3901, May 1991
Biophysics

Bursting electrical activity in pancreatic β cells caused by Ca^{2+}- and voltage-inactivated Ca^{2+} channels

JOEL KEIZER[†‡] AND PAUL SMOLEN[†§]

[†]Institute of Theoretical Dynamics and [‡]Department of Chemistry, University of California, Davis, CA 95616

Communicated by Terrell L. Hill, January 15, 1991 (received for review September 26, 1990)

ABSTRACT **We investigate the hypothesis that two classes of Ca^{2+} currents, one quickly inactivated by Ca^{2+} and one slowly inactivated by voltage, contribute to bursting electrical activity in pancreatic islets. A mathematical model of these currents is fit to the experimental whole-cell current–voltage and inactivation profiles, thereby fixing the Ca^{2+} conductance and all activation and inactivation parameters. Incorporating these currents into a model that includes delayed rectifier K^+ channels and ATP-sensitive K^+ channels, we show that only abnormal bursting is obtained. Modification of activation parameters to increase Ca^{2+} channel open times, as suggested by experiment, yields a more robust bursting similar to that observed in intact islets. This reinforces the suggestion that in addition to ATP-sensitive K^+ channels, Ca^{2+} channels may serve as glucose sensors in the β cell.**

I. Introduction

Pancreatic β cells, when perifused in islets with physiological glucose concentrations that induce insulin secretion, also exhibit a rhythmic electrical activity called bursting (1–7). Several K^+ and Ca^{2+} ion channels have been implicated in bursting. Voltage-gated K^+ and Ca^{2+} channels are thought to be responsible for the action potential spikes (8), while Ca^{2+}-activated K^+ channels (KCa) (9) and ATP-sensitive K^+ channels (KATP) (10, 11) have been proposed as "trigger" or "pacemaker" channels. Mathematical models that include the voltage-gated channels and one or both of the trigger channels have shown that both mechanisms can support bursting (12, 13). Recent experimental evidence, however, has called into question the relevance of both KCa channels and KATP channels. Indeed, Kukuljan *et al.* (14) have shown that charybdotoxin, which specifically inhibits KCa channels in the β cell, has no effect on bursting, while Smith *et al.* (15) conclude that the total KATP conductance changes by <10 pS per cell, a value that may be too small to account for repolarization. Furthermore, isolated β cells and small clusters can support bursting more regular than can be accounted for by the small number of active KCa and KATP channels in single cells.

Recently, Satin and Cook (16, 17) have proposed that slow voltage inactivation of Ca^{2+} channels might be involved in repolarization of the bursts. In addition to the fast (order of 75 ms) Ca^{2+} inactivation of Ca^{2+} channels (18), they report evidence for voltage inactivation of calcium current on the time scale of 1–10 s. Similar results are found in both HIT cells (17) and cultured adult mouse cells (18), both of which exhibit bursting-type electrical activity and insulin secretion. Satin and Cook interpret their Ca^{2+} currents in terms of distinct fast Ca^{2+}-inactivated and slow voltage-inactivated channels. In this paper, we develop a mathematical model of these currents, which we combine with the delayed rectifier K^+ current (8) and a KATP current (15) to examine whole-cell electrical activity and bursting.

II. HIT Cell Model for Ca^{2+} Currents

The mathematical model developed in this section includes two Ca^{2+} currents and two K^+ currents. The calcium currents correspond to the fast Ca^{2+}-inactivated and slow voltage-inactivated Ca^{2+} channels found by Satin and Cook (17) in HIT cells (19, 20), while the K^+ currents are due to the K^+ delayed rectifier (8) and KATP channels with a constant conductance whose value is set by the ATP/ADP ratio (21). The K^+ delayed rectifier has been analyzed by Sherman *et al.* (22), who assigned it a maximal conductance of 2500 pS per cell and the activation parameters in the *Appendix*. The magnitude of the KATP conductance in mouse β cells has been estimated to be 360 pS per cell in the presence of 8 mM glucose (23). We use conductance values of this order in our calculations and a K^+ reversal potential of −75 mV (12, 13, 22). Standard values of the capacitance and cell area have been adopted (22).

According to Satin and Cook (17), the whole-cell Ca^{2+} current consists of contributions from two classes of channels, which we write in the Goldman–Hodgkin–Katz form

$$I_{Ca} = g_{Ca}Ca_oV/[1 - \exp(2FV/RT)], \quad [1]$$

where V is the membrane potential, RT/F is the usual thermal voltage, Ca_o is the external Ca^{2+} concentration (mM), and g_{Ca} is the conductance·mM^{-1}, written as

$$g_{Ca} = \bar{g}_{Ca}[PO_f \cdot X_f + m_s^\infty(V)J(1 - X_f)]. \quad [2]$$

The first term in Eq. 2 represents the conductance of the fast Ca^{2+}-inactivated Ca^{2+} channels, which carry a fraction X_f of the maximal conductance, $\bar{g}_{Ca}$. We use the domain model of Sherman *et al.* (24) to describe Ca^{2+} inactivation. [See the *Appendix*, where PO_f is the fraction of open channels, O, in the scheme (**A5**) and I is the state inactivated by the voltage-dependent calcium concentration at the mouth of open channels, $Ca_d(V)$.] The second term in Eq. 2 is the slow voltage-inactivated Ca^{2+} conductance, for which $m_s^\infty(V)$ is the steady-state activation (assumed rapid), and J is the voltage-dependent inactivation, which relaxes to its voltage-dependent steady-state value, $J^\infty(V)$, according to

$$dJ/dt = -[J - J^\infty(V)]/\tau_J(V), \quad [3]$$

with the voltage-dependent time constant, τ_J.

The usual Boltzmann functional form is assumed for the activation, $m_s^\infty(V)$. Based on Satin and Cook's observations (17), the half-activation voltage is shifted 10 mV positive from that for the steady-state activation, $m_f^\infty(V)$, for the fast Ca^{2+}-inactivated channels. Boltzmann-type formulas are also assumed for the steady-state inactivation, $J^\infty(V)$, and the

The publication costs of this article were defrayed in part by page charge payment. This article must therefore be hereby marked "*advertisement*" in accordance with 18 U.S.C. §1734 solely to indicate this fact.

§Present address: Mathematical Research Branch, Building 31, Room 4B-54, National Institutes of Health, Bethesda, MD 20892.

inactivation time, $\tau_J(V)$. Details of the functional forms and parameters are given in the *Appendix*.

To describe the time course of the whole-cell voltage and current we use the differential equation (12, 25, 37)

$$CdV/dt = -\sum_i I_i, \quad [4]$$

where C is the capacitance and the sum is over the appropriate ion currents. To fix parameter values for the Ca^{2+} channels, the Ca^{2+} current in Eqs. **1** and **2** is used by itself in this expression. To analyze bursting activity, the KATP and delayed rectifier K^+ currents in the *Appendix* are also added to the right-hand side of Eq. **4**.

We have used the results of Satin and Cook's experimental activation and inactivation measurements (17) to fit the parameters of the two Ca^{2+} currents described above. We have simulated three key types of experiments: (*i*) 40-ms and 10-s voltage clamp experiments at various test potentials starting from a holding potential of −100 mV (to determine peak *I–V* relationships and time course of activation and inactivation); (*ii*) three-pulse protocols to measure inactivation due to 40-ms and 10-s conditioning at fixed potential; and (*iii*) 100-ms conditioning pulses at +10 mV to measure the *I–V* relationship for the slowly inactivating current.

To simulate the first type of experiment, we utilized Eq. **4**, supplemented with Eqs. **1–3** and the dynamical equations for fast Ca^{2+} inactivation of Sherman *et al.* (24). The resulting peak *I–V* curve in 40-ms voltage clamp is shown in Fig. 1*A*. The maximal current of −65 pA and the general shape of the curve below +50 mV is similar to that shown in figure 2*B* of Satin and Cook (17). With the "standard" parameter values given in Fig. 1, we obtain somewhat higher currents below −40 mV than were shown experimentally. This may be due in part to the experimental method of leak subtraction since Plant (18) finds somewhat larger fractional currents in this range using 10 mM external Ca^{2+}. The complete current time records of these 40-ms simulations (data not shown) are similar in time scale and magnitude to the data of Satin and Cook (17). It should be noted that the measured inactivation rates in HIT cells are faster than the rates measured in mouse β cells (18, 26). To account for this, as well as for the fact that HIT inactivation is not lost after holding for 100 ms at −100 mV, the inactivation rate constant, k^+, has been increased to 4 times the value used by Sherman *et al.* (24) and the reactivation rate constant, k^-, was decreased by nearly an order of magnitude (see *Appendix*).

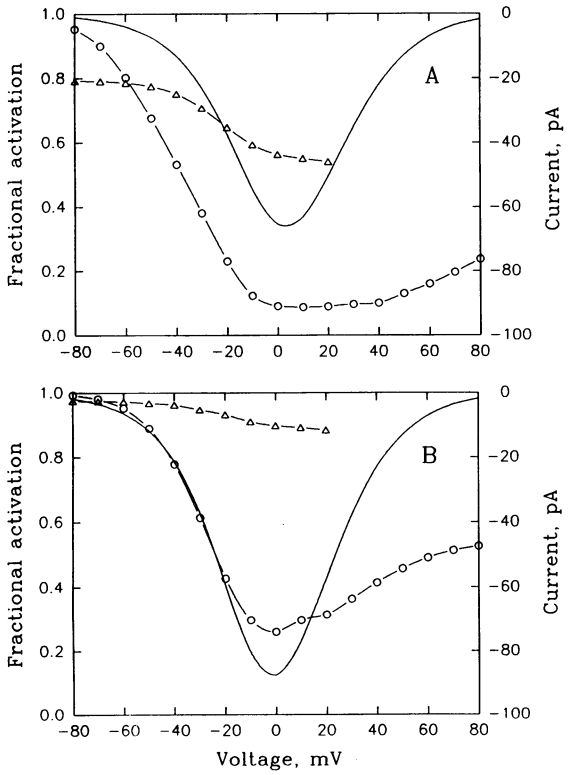

FIG. 1. Simulated peak *I–V* curves (solid line), and simulated inactivation curves determined via the three-pulse protocol incorporating either a 40-ms (triangles) or 10-s (circles) conditioning pulse. (*A*) Results with the standard parameter set found to best reproduce HIT cell data: $V_{mf} = -3$ mV, $S_{mf} = 10$ mV, $V_j = -40$ mV, $S_j = 7$ mV, $V_{ms} = 7$ mV, $S_{ms} = 14$ mV, $Ca_o = 3$ mM, $k^- = 0.002$ ms^{-1}, $k^* = 7.56 \times 10^{-4}$ ms^{-1}·mM^{-1}·mV^{-1}, $X_f = 0.45$, $\bar{g}_{Ca} = 3.92 \times 10^3$ pS·mM^{-1}, and $\tau_J = 30$ s. (*B*) Results with the modified parameter set that gives good bursting electrical activity; the differences from *A* are $k^* = 4.73 \times 10^{-5}$ ms^{-1}·mM^{-1}·mV^{-1}, $V_{mf} = -8$ mV, $V_{ms} = +2$ mV.

Good fits to the 10-s voltage clamp time records (figure 2*A* in ref. 19), which show inactivation on the 1- to 7-s time scale, are also obtained with the standard parameters given in Fig. 1. In good agreement with their measurements, the relaxation time τ_J is 0.84 s at $V = +10$ mV and 7.0 s at $V = -20$ mV.

Theoretical results for the 40-ms and 10-s inactivation curves based on the standard parameter set are also shown in Fig. 1. The protocol used for the simulations mimicked the three-pulse protocol of Satin and Cook (17)—namely, holding at −100 mV followed by a 10-ms pulse at +10 mV; 150 ms at −100 mV; 40 ms (or 10 s) at the conditioning potential; 40 ms at −100 mV; and a final 10-ms pulse at +10 mV. The peak currents in the first (I_{P1}) and final (I_{P2}) pulses to +10 mV were recorded, and the fraction of channels not inactivated (h) was estimated from the formula $h = I_{P2}/I_{P1}$ (18). We show results for the 40-ms simulations only for potentials less than +20 mV since at higher potentials our theoretical expression for $\tau_J(V)$ becomes significantly smaller than the limiting value of 1 s reported experimentally (17). This leads to significant inactivation of the slow-voltage inactivated current above +20 mV even on the 40-ms time scale and, thus, to spurious results. In the physiological region below +20 mV our 40-ms inactivation curves reproduce the correct amount of maximal inactivation (45%) and the overall shape of the inactivation curves. Indeed, our simulations even capture the residual, nearly constant, level of inactivation below −50 mV that is seen experimentally. According to our calculations this is not due to inactivation of the slow current, as speculated by Satin and Cook (17), but rather to the kinetics of inactivation of the fast-inactivated channels.

Our simulations of the 10-s inactivation protocol show good agreement with experiments at all values of potential (figure 4*B* in ref. 17). The increase in inactivation on this time scale between −80 and 0 mV is the sum of the steady-state voltage inactivation, $J^\infty(V)$, and the steady-state fast Ca^{2+} inactivation, $h_f(V)$ (see *Appendix*). Positive to 0 mV, the steady-state value of $J^\infty(V)$ is essentially 0 and the decline of inactivation (seen both in Fig. 1*A* and the experiment) is due to a lengthening of the transition time from the open state to the inactivated state as the potential approaches the reversal potential of Ca^{2+}.

As a final check on our Ca^{2+} currents, we carried out 100-ms conditioning pulses at +10 mV, followed by 40 ms holding at −100 mV, and we measured the peak *I–V* curve of the remaining current at various test voltages. The resulting *I–V* curve (data not shown) is shifted ≈10 mV to the right and decreased in magnitude by almost exactly 50% compared to the unconditioned *I–V* curve in Fig. 1*A*. This also is in good agreement with Satin and Cook (17) (cf. their figure 8*B*). Our simulation results for the conditioned *I–V* curve are within 10% of the theoretical curve obtained by setting $PO_f = 1.3 \times 10^{-3}$ and $J = 0.90$ in Eqs. **1** and **2**, the values achieved after conditioning. This lends support to the idea that conditioning

at +10 mV predominantly inactivates the fast Ca^{2+}-inactivated channel.

While our standard set of Ca^{2+} channel parameters leads to good agreement with Satin and Cook's HIT cell experiments (17), we have not attempted to fit the data to better than 5–10%. We have settled on this degree of accuracy because the experiments show a great deal of natural variation from cell to cell. In an effort to reduce the juggling of parameters, we have fixed many of them to agree with previous work (22, 24) and focused on obtaining a good set of parameters for the slow channel, the maximal current fraction of the fast channels, and kinetic parameters for Ca^{2+} inactivation of the fast channels. We note that previous attempts (27, 28) to explore bursting in the β cell by using slow voltage-inactivating Ca^{2+} channels have employed parameters at serious odds with both HIT and mouse cell experiments—e.g., a shift of the slow voltage activation 25–28 mV *negative* rather 10 mV *positive* of the fast voltage inactivation (28, 29).

III. Analysis of Whole-Cell Electrical Activity

To analyze whole-cell electrical activity we used the fast and slow Ca^{2+} currents given in Eqs. **1–3** along with the delayed rectifier K^+ and ATP-sensitive K^+ currents described in the *Appendix*. Having fixed the parameters of the Ca^{2+} currents, the primary parameters varied in this section are τ_n, the rate of activation of the delayed rectifier, and the total conductance of the ATP-sensitive K^+ channel, G_{ATP}. We justify this based on the facts that the rate of activation of the delayed rectifier is known to be temperature dependent (30), while G_{ATP} is a function of glucose concentration (10, 11). While the maximal value of G_{ATP} in the absence of glucose has been estimated to be 5100 pS in mouse β cells, it is reduced by some 80–90% in the presence of 8 mM glucose (15). In our simulations, a gradual reduction of G_{ATP} through this range leads to a slow depolarization of the membrane potential from −75 mV to −68 mV. Reduction of G_{ATP} further to 235 pS depolarizes the cell to −56 mV. Just below this value of G_{ATP}, the membrane potential exhibits a kind of rhythmic, bursting electrical activity.

While the time course of bursting depends somewhat on the magnitude of the activation rate of the delayed rectifier, τ_n, bursting consists, essentially, of two "silent" states, one near −60 mV and another near −35 mV. The transition between the hyperpolarized and depolarized states is accompanied by vestigial spikes of decreasing amplitude when τ_n = 20 ms. When τ_n is increased to 30 ms the spikes become somewhat more pronounced, as shown for a G_{ATP} value of 180 pS in Fig. 2*A*. This general picture is not modified if the maximal conductance of the delayed rectifier, G_K, is decreased from its "standard" value of 2500 pS to as small a value as 500 pS or increased to 5000 pS. Thus, we conclude that this generic behavior, including the anomalous bursting, is dominated by the electrical properties of the two calcium currents.

This type of bursting is abnormal and has not been reported for β cells under physiological conditions (31). Nonetheless, it can be understood easily by using the same type of mathematical analysis that was used for previous models of β-cell electrical activity (38). Analysis of the "fast" dynamics of the voltage, V, using the "slow" inactivation, $1 - J$, as a parameter reveals a z-shaped curve of steady states with the following features: (*i*) a depolarized (upper) branch of stable steady states that are approached in an oscillatory fashion; (*ii*) a hyperpolarized (lower) branch of steady states that are exponentially stable; and (*iii*) an intermediate branch of steady states that are unstable. For the standard parameters (see Fig. 1), there is a Hopf bifurcation leading to stable oscillations on the upper branch at positive values of $1 - J$ below 0.18. Viewed in this fashion, the abnormal bursts

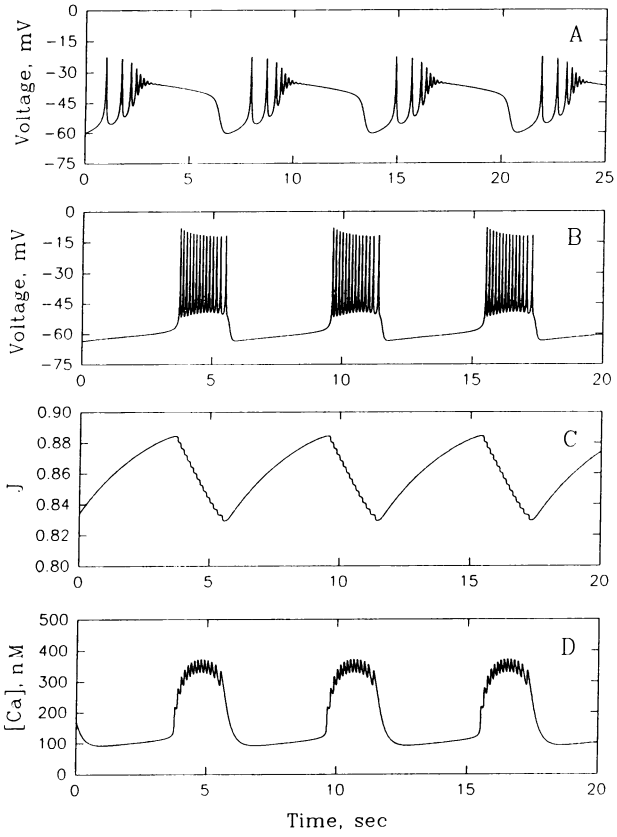

FIG. 2. Simulated time courses for membrane potential, fractional activation of slow calcium channels (J), and cytoplasmic free calcium concentration. (*A*) Standard parameter set for the Ca^{2+} channels used in Fig. 1*A*, G_{ATP} = 180 pS, and τ_n = 30 ms. (*B–D*) Modified parameter set (see Fig. 1*B*) with G_{ATP} = 380 pS, τ_n = 20 ms, k_{CA} = 0.24 ms^{-1}, and f = 0.015.

consist of three distinct portions. First, a short hyperpolarized phase on the lower branch. As $1 - J$ decreases, this evolves into several large spikes that depolarize the membrane sufficiently to cause the slow inactivation $1 - J$ to begin increasing near the upper branch. Since the upper branch supports only damped oscillations, the cycle is completed when $1 - J$ exceeds the value at the right "knee" of the z curve and then rapidly repolarizes to the lower branch. The major distinctions between this type of bursting behavior and that seen in other models are the large spikes emanating from the lower branch and the damped oscillations on the upper branch. These differences can be shown to arise from the fast Ca^{2+} inactivation in this model, which relaxes on a time scale intermediate between that of the voltage and the slow voltage inactivation. The details of this analysis will be given elsewhere.

IV. Modification of Ca^{2+} Currents and Normal Bursting

Because the HIT cell Ca^{2+} currents do not explain the electrical activity observed in the β cells (2, 15, 39), we have sought modifications in both the K^+ and Ca^{2+} currents that might lead to normal bursting. Changes in the magnitude of the conductances of either the delayed rectifier or the ATP-sensitive channel do not help in this regard, nor does increasing (or decreasing) the relaxation time, τ_n, of the delayed rectifier or changing its activation parameters. Experiments by Smith *et al.* (15), however, suggest that 20 mM glucose increases the activity of individual Ca^{2+} channels and lengthens their mean open time. This is reversed by inhibitors of glucose metabolism, suggesting involvement of a metabolic intermediate. It is also possible that increasing the temper-

ature causes changes in Ca^{2+} channel parameters. Indeed, several groups have noted that both electrical activity (32) and intracellular Ca^{2+} oscillations (34) are abolished at room temperature, where Satin and Cook's experiments were performed.

Thus, we checked whether increasing open times or decreasing the time spent in the inactivated state would modify whole-cell electrical activity. To this end, we modified the standard activation parameters for the Ca^{2+} currents by shifting the half-maximal voltage to lower potentials and increasing the slope at half-maximum. Changes in the opposite direction were investigated for inactivation parameters. The rate constant, k^+, for the fast Ca^{2+} inactivation step (see *Appendix*) was also decreased. The vast majority of these changes had no significant effect on bursting in the sense that values of G_{ATP} and τ_n in the physiologically reasonable range led only to abnormal bursts like those in Fig. 2*A*.

We found that shifting the half-maximal activation of both Ca^{2+} currents by -5 mV and decreasing the rate constant for inactivation, k^+, by a factor of 16 led to the apparently normal bursts in Fig. 2*B*. The bursting period ($\approx$6 s) is somewhat shorter than seen experimentally (2), while spiking frequency ($\approx$6 s^{-1} decreasing to 3 s^{-1}) is similar to that normally observed. The two parameter changes have the effect of increasing the open time for both Ca^{2+} currents, although they affect most strongly the fast Ca^{2+}-inactivated current. This is illustrated in Fig. 1*B*, in which the current and fractions not inactivated should be compared to Fig. 1*A* for the standard parameters. These parameter changes reduce the maximal inactivation in the 40-ms experiment from 45% to 10% and substantially reduce the inactivation in the 10-s experiments. The maximal current is seen to be increased by $\approx$40% by these changes. We have found that smaller changes than this do not lead to bursting, but only to an exaggerated form of the abnormal bursting with more spikes during the transition to the depolarized state. Although the two changes that give rise to the modified standard parameter set are relatively minor, it is clear from comparing Fig. 1*B* with the results of Satin and Cook (17) that the resulting modified inactivation curves lie well outside experimental error. We conclude, therefore, that experimentally significant reductions in the Ca^{2+} inactivation observed for HIT cells would be required to allow slow voltage inactivation to produce bursting.

Chay (28, 29) has suggested that the half-maximal inactivation potential of a slow current, V_j, could be effective in modulating the duration of the active (spiking) phase of a burst. We have verified this to be the case for the modified parameter set. Indeed, when V_j is reduced from -40 mV to -28.6 mV, the percentage active phase increases continuously from about 37% to 90%, while the period increases from 5.9 s to a maximum of $\approx$10.4 s before continuous spiking abruptly occurs.

The period, τ, of both the abnormal bursts and the normal bursts in Fig. 2 are determined predominantly by the size of $\tau_J(V)$. The period appears to be roughly the size of τ_J at -20 mV—e.g., $\approx$7 s for the modified parameter set. Indeed, we noted above that as V_j is increased, the period increases—approximately in accord with the relationship $\tau = \tau_J$ (-20 mV). Thus, significant increases in the bursting period beyond 10 s would require significant slowing of the slow voltage inactivation process. Experimentally there is great variation in the period of bursting and periods of >120 s have been observed in both islets (2) and whole-cell records (15). To explain this fact by slow voltage inactivation alone would require an order of magnitude increase in the measured time constants for slow voltage inactivation.

It is interesting that the modified value of G_{ATP} that leads to normal bursting is 380 pS, close to the value estimated by Ashcroft and Smith (23) for the conductance of mouse β cells in 8 mM glucose. In our calculations, increases in G_{ATP} displace the z curves to the left, leading to a stable hyperpolarized state, as described in the previous section. Small decreases in G_{ATP} from its modified standard value of 380 pS—e.g., to 340 pS—however, lead to abnormal bursting not unlike that shown in Fig. 2*A*. This change, however, is more "normal" (32) in that normal bursting can be recovered by a small increase in τ_n (e.g., from 20 ms to 20.7 ms). This is caused by a shift in the Hopf bifurcation point on the upper branch, whose location is sensitive to both G_{ATP} and τ_n. Larger values of τ_n—e.g., 22 ms—shift the Hopf bifurcation curve so far to the left that only the "beating" type spiking is observed.

V. Discussion

The main objective of this work was to determine whether the slow voltage inactivation of HIT cell Ca^{2+} currents could suffice to produce bursting. The answer is a qualified "yes," since without specific reduction in Ca^{2+} inactivation and increased Ca^{2+} activation only abnormal bursts are observed. These modifications are in line with the observations of Ashcroft and Smith (15) that glucose increases Ca^{2+}-channel activity. Despite the fact that 11 mM glucose is present in the bathing solutions of Satin and Cook (17), it is possible that in their whole-cell configuration a glycolytic intermediate (or a protein that might, for example, phosphorylate Ca^{2+} channels) washed out of the cell. Another possibility is that the modifications necessary to achieve normal bursting might be caused by increasing the temperature from 20°C to 22°C into the physiological range where bursting occurs (22). It is also interesting to note that mouse β cells exhibit somewhat less inactivation than HIT cells (26). This appears to be due primarily to a slower inactivation time course for the fast Ca^{2+}-inactivated channels, which in mouse carry only 36% of the maximal current (26). These modifications are in the same direction that we have had to modify the HIT cell data to achieve normal bursting. In this regard, it is also interesting to note that Rojas *et al.* (35) have presented evidence for a Ca^{2+} channel activated by glucose in human β cells. If present in mouse and HIT cells, this channel might also suffice to provide the additional Ca^{2+} current needed to achieve bursting.

Increasing the half-maximal inactivation potential, V_j, of the slow voltage-inactivated current provides another possible link between Ca^{2+} currents and glucose. As we have mentioned, increasing V_j increases the percentage active phase, ultimately leading to continuous spiking. This mimics the effects of increased glucose concentrations in perifused islets, as does the fact that the bursting period, τ, increases only slightly (36). The short bursting period (6–10 s) is a problematic feature of the slow voltage inactivation model. Data from mouse cells (26), which have a comparable voltage inactivation time, are of no help here, nor is an increase in temperature, which should only decrease relaxation times. Thus for slow voltage inactivation alone to serve as the trigger for bursting would require an increase of at least a factor of 2 or more in relaxation time.

A new feature of our slow voltage inactivation mechanism is that it is independent of intracellular Ca^{2+}. As a consequence, intracellular Ca^{2+} concentrations do not necessarily have to change slowly in this model. This is important since Valdeomillos *et al.* (3) have observed that intracellular Ca^{2+} increases quite rapidly on the upswing of Ca^{2+} oscillations in islets. We can account for this in the present model by using the simple Ca^{2+} balance equation

$$f^{-1}dc/dt = -\gamma I_{Ca} - k_{Ca}c, \qquad [5]$$

where c is the concentration (μM) of free intracellular Ca^{2+}, f is the fraction of free Ca^{2+}, $\gamma = 4.50 \times 10^{-6}$ converts fA to $\mu M \cdot ms^{-1}$, and k_{Ca} is a first-order rate constant for extrusion of Ca^{2+} from the cytosol. Eq. 5 is coupled to the voltage via I_{Ca} and, when solved numerically by the modified parameter set and $k_{Ca} = 0.24\ ms^{-1}$, $f = 0.015$, yields the intracellular Ca^{2+} oscillations shown in Fig. 2D. The rapid increase in c at the onset of the active phase is like that seen experimentally (2) and unlike that obtained in previous models (12, 13, 27).

Another interesting feature of the present bursting mechanism is that it invokes two types of glucose sensors. First, the ATP-sensitive K^+ channel is used to depolarize the cell into the region of the z curve where bursting is possible. And second, reduction of the Ca^{2+} inactivation and increase in the activation of both Ca^{2+} channels is used to initiate normal bursting and modulate the percentage active phase. Whether these features, or something similar, turn out to be compatible with future experimental work remains to be seen.

Appendix: Functional Forms and Definition of Parameters

Boltzmann-type equations are assumed for all steady-state activation (m_f^∞, m_s^∞, n^∞) and inactivation (J^∞) functions. For example, for the fast Ca^{2+} activation

$$m_f^\infty(V) = 1/[1 + \exp(V_{mf} - V)/S_{mf}], \quad \text{[A1]}$$

and for the slow voltage inactivation

$$J^\infty(V) = 1/[1 + \exp(V - V_j)/S_j], \quad \text{[A2]}$$

with comparable notation for m_s^∞ and n^∞.

The delayed rectifier current is taken from Sherman *et al.* (24) as $I_{KV} = g_K n(V - V_K)$, with n solving

$$dn/dt = -[n - n^\infty(V)]/\tau_n(V). \quad \text{[A3]}$$

The relaxation time for the delayed rectifier is

$$\tau_n(V) = \tau_n/\{\exp[V - V_n)/65] + \exp[(-V + V_n)/20]\}. \quad \text{[A4]}$$

The ATP-sensitive K^+ current is written as $G_{KATP}(V - V_K)$.

Kinetic parameters for the domain model of fast Ca^{2+} inactivation follow the notation of Sherman *et al.* (24). Thus, in the mechanism

$$C \underset{\beta}{\overset{\alpha}{\rightleftarrows}} O \underset{k^-}{\overset{k^+Ca_d(V)}{\rightleftarrows}} I, \quad \text{[A5]}$$

$\alpha(V) = 0.78\ m_f^\infty(V)$, $\alpha + \beta = 0.78$ (both in ms), and

$$k^+Ca_d(V) = k^*Ca_o V/[1 - \exp(2FV/RT)], \quad \text{[A6]}$$

with $RT/2F = 13.35$ mV. The units of k^* are $ms^{-1} \cdot mM^{-1} \cdot mV^{-1}$ and k^- units are ms^{-1}. The theoretical expression for the fraction not inactivated, $h_f(V)$, for the fast Ca^{2+} inactivation in the domain model is (24)

$$h_f(V) = 1/[1 + k^+Ca_d(V)m_f^\infty(V)/k^-]. \quad \text{[A7]}$$

The slow voltage inactivation J satisfies Eq. 3, with $\tau_J(V)$ defined by the symmetrical Boltzmann formula

$$\tau_J(V) = \tau_J/\{\exp[(V - V_j)/2S_j] + \exp[-(V - V_j)/2S_j]\}. \quad \text{[A8]}$$

Other parameters that were generally fixed in this work (22) were $V_K = -75$ mV, $g_K = 2500$ pS, $C = 5310$ fF, $V_{cell} = 2301\ \mu m^3$, $S_n = 5.6$ nV, $V_n = -13$ mV.

This work was supported by National Science Foundation Grant DIR-90-06104 and the Agricultural Experiment Station of the University of California, Davis.

1. Dean, P. M. & Matthews, E. K. (1970) *J. Physiol. (London)* **210,** 225–264.
2. Atwater, I., Dawson, C. M., Scott, A., Eddlestone, G. & Rojas, E. (1980) *Biochemistry and Biophysics of the Pancreatic β-Cell* (Thieme, New York), pp. 100–107.
3. Valdeomillos, M., Santos, R. M., Contreras, D., Soria, B. & Rosario, L. M. (1989) *FEBS Lett.* **259,** 19–23.
4. Draznin, B. & Dahl, R. (1989) in *Molecular and Cellular Biology of Diabetes Mellitus*, eds. Draznin, B., Melmed, S. & LeRoith, D. (Liss, New York), Vol. 1, pp. 37–48.
5. Boyd, A. E., III, Rojan, A. S. & Gaines, K. L. (1989) in *Molecular and Cellular Biology of Diabetes Mellitus*, eds. Draznin, B., Melmed, S. & LeRoith, D. (Liss, New York), Vol. 1, pp. 93–106.
6. Meissner, H. (1976) *J. Physiol. (Paris)* **72,** 757–769.
7. Atwater, I., Rojas, E. & Scott, A. (1979) *J. Physiol. (London)* **291,** 57P (abstr.).
8. Rorsman, P. & Trube, G. (1986) *J. Physiol. (London)* **374,** 531–547.
9. Atwater, I., Dawson, C., Ribalet, B. & Rojas, E. (1979) *J. Physiol. (London)* **288,** 575–593.
10. Cook, D. & Hales, C. N. (1984) *Nature (London)* **311,** 271–273.
11. Ashcroft, F., Harrison, D. & Ashcroft, S. (1984) *Nature (London)* **312,** 446–448.
12. Chay, T. & Keizer, J. (1983) *Biophys. J.* **42,** 181–190.
13. Keizer, J. & Magnus, G. (1989) *Biophys. J.* **56,** 229–242.
14. Kukuljan, M., Goncalves, A. A. & Atwater, I. (1991) *J. Membr. Biol.* **119,** 187–195.
15. Smith, P. A., Ashcroft, F. & Rorsman, P. (1990) *FEBS Lett.* **261,** 187–190.
16. Satin, L. S. & Cook, D. L. (1988) *Pflügers Arch.* **411,** 401–409.
17. Satin, L. S. & Cook, D. L. (1989) *Pflügers Arch.* **414,** 1–10.
18. Plant, T. D. (1988) *J. Physiol. (London)* **404,** 731–747.
19. Boyd, A. E., III, Hill, R. S., Oberwetter, J. M. & Berg, M. (1986) *J. Clin. Invest.* **77,** 774–781.
20. Keahey, H., Rajan, A. S., Boyd, A. E., III, & Kunze, D. L. (1989) *Diabetes* **38,** 188–193.
21. Misler, S., Falke, L. C., Gillis, K. & McDaniel, M. L. (1986) *Proc. Natl. Acad. Sci. USA* **83,** 7119–7123.
22. Sherman, A., Rinzel, J. & Keizer, J. (1988) *Biophys. J.* **54,** 411–425.
23. Ashcroft, F. M. & Smith, D. A. (1989) *J. Physiol. (London)* **417,** 79P (abstr.).
24. Sherman, A., Keizer, J. & Rinzel, J. (1990) *Biophys. J.* **58,** 985–995.
25. Keizer, J. (1988) *Math. Biosci.* **90,** 127–138.
26. Hopkins, W. F., Satin, L. S. & Cook, D. L. (1991) *J. Membr. Biol.* **119,** 229–239.
27. Chay, T. R. & Cook, D. L. (1988) *Math. Biosci.* **90,** 139–153.
28. Chay, T. R. (1990) *Am. J. Physiol.* **258,** C955–C965.
29. Chay, T. R. (1990) *J. Theor. Biol.* **142,** 305–315.
30. Hille, B. (1984) *Ionic Channels in Excitable Membranes* (Sinauer, Sunderland, MA), p. 330.
31. Ribalet, B. & Biegelman, P. M. (1981) *Am. J. Physiol.* **241,** C59–C67.
32. Atwater, I., Goncalves, A., Herchuelz, A., Lebrun, P., Malaisse, W. J., Rojas, E. & Scott, E. (1984) *J. Physiol. (London)* **348,** 615–627.
33. Falke, L. C., Gillis, K. D., Pressel, D. M. & Misler, S. (1989) *FEBS Lett.* **251,** 167–172.
34. Hellman, B., Gylfe, E., Grapengiesser, E., Panten, U., Schwanstecher, C. & Heipel, C. (1990) *Cell Calcium* **11,** 413–418.
35. Rojas, E., Hidalgo, J., Carroll, P. B., Li, M.-X. & Atwater, I. (1990) *FEBS Lett.* **261,** 265–270.
36. Meissner, H. P. & Atwater, I. (1976) *Horm. Metab. Res.* **8,** 11–16.
37. Plonsey, R. (1969) *Bioelectric Phenomena* (McGraw Hill, New York).
38. Rinzel, J. (1985) in *Ordinary and Partial Differential Equations*, eds. Sleeman, B. D. & Jarvis, R. J. (Springer, New York), pp. 304–316.
39. Atwater, I., Carroll, P. & Li, M.-X. (1989) in *Molecular and Cellular Biology of Diabetes Mellitus*, eds. Draznin, B., Melmed, S. & LeRoith, D. (Liss, New York), pp. 49–68.